Oil & Natural Gas Technology

DOE Award No.: DE-FE0001243

Topical Report

DEVELOPMENT OF CFD-BASED SIMULATION TOOLS FOR IN SITU THERMAL PROCESSING OF OIL SHALE/SANDS

Submitted by:
University of Utah
Institute for Clean and Secure Energy
155 South 1452 East, Room 380
Salt Lake City, Utah 84112

Prepared for:
United States Department of Energy
National Energy Technology Laboratory

February 2012

Office of Fossil Energy

TOPICAL REPORT:

DEVELOPMENT OF CFD_BASED SIMULATION TOOLS FOR IN SITU THERMAL PROCESSING OF OIL SHALE/SANDS

Authors: Michal Hradisky and Philip J. Smith

DOE Award No.: DE-FE0001243

Reporting Period: October 1, 2009 – September 30, 2011

Report Issued: February 2012

Submitted by:
University of Utah
Institute for Clean and Secure Energy
155 South 1452 East, Room 380
Salt Lake City, UT 84112-0190

Prepared for:
United States Department of Energy
National Energy Technology Laboratory

DISCLAIMER

ABSTRACT

In our research, we are taking the novel approach of developing and applying high performance computing, computational fluid dynamics (CFD)-based simulation tools to a modified in-situ process for production of oil from oil shale. The simulation tools being developed capture the relevant physical processes and data from a large-scale system. The modified in-situ application is a pilot-scale heat transfer process inside Red Leaf Resources' EcoShale capsule. We demonstrate the need to understand fluid flow behavior in the convective channels of the rubblized shale bed as convective heating greatly decreases the time required to heat the oil shale to the production temperature when compared with conductive heating alone. We have developed and implemented a geometry creation strategy for a representative section of the EcoShale capsule, developed a meshing approach to deal with the complicated geometry and produce a well-behaved mesh, analyzed the effects of boundary conditions on the simulation results, and devised a new operator splitting solution algorithm that reduces computational costs by taking advantage of the differing convective and conductive time scales occurring in the simulation. These simulation tools can be applied to a wide range of processes involving convective fluid flow heating in rubblized beds.

TABLE OF CONTENTS

LIST OF FIGURES

INTRODUCTION

In-situ technologies are currently being explored because of their potential for reducing the environmental footprint of oil shale development. However, the first generation technologies have proven to be energy-intensive, and many unknowns remain relative to optimal heating strategies, potential groundwater contamination, and achievable production rates.

Reservoir simulation tools are typically applied to in-situ production processes. However, in the case of a modified in-situ process, there is a distribution of rock size in the production bed and those rocks are packed in such a way that large convective currents heat the bed. Preliminary simulations of a modified in situ process using a reservoir simulation-type approach (e.g. fluid flow through porous media) showed that such an approach is insufficient to resolve key physics affecting production rates, particularly convective heat flow patterns.

We are taking the novel approach of applying CFD-based simulation tools to a modified in-situ process. Rigorous validation/uncertainty quantification (V/UQ) of this approach requires both a simulation tool that captures the relevant physical processes and data from a large-scale system. Initially, we are focusing on creating simulations of the pilot-scale heat transfer process inside Red Leaf Resources' EcoShale capsule. The tools being developed can be applied to a wide range of processes involving convective fluid flow/heating in rubblized beds.

PROJECT DESCRIPTION

The EcoShale In-Capsule Technology has been developed by Red Leaf Resources, Inc. to produce high quality liquid fuels from oil shale economically and with a minimal environmental impact. The process comprises heating mined and rubblized oil shale using pipes fired with natural gas burners in a clay-lined, closed-surface capsule. This technology does not require process water, protects ground water by using a liner inside the capsule, and allows for rapid site reclamation by providing an overburden over the capsule [1]. The process schematic is shown in Figure 1.

Software Tools

In the early stages of this project, we anticipated creating a Large Eddy Simulation (LES) tool based on the ARCHES platform (a highly scalable, finite-volume LES code developed at the Institute for Clean and Secure Energy) that used a statistical approach to model geometry consisting of voids and physical pieces of shale. It was later determined that a simulation involving the actual geometry of shale pieces would provide a better representation of this process. The commercially available simulation software Star-CCM+, created by CD-adapco, has been developed to handle complex geometries and can be used to model the convective currents through the channels of the rubblized bed. Scaling studies performed on Star-CCM+

showed reasonable scalability up to 768 processes. Because of these capabilities, we determined that Star-CCM+ would be a more appropriate tool to achieve our project objectives.

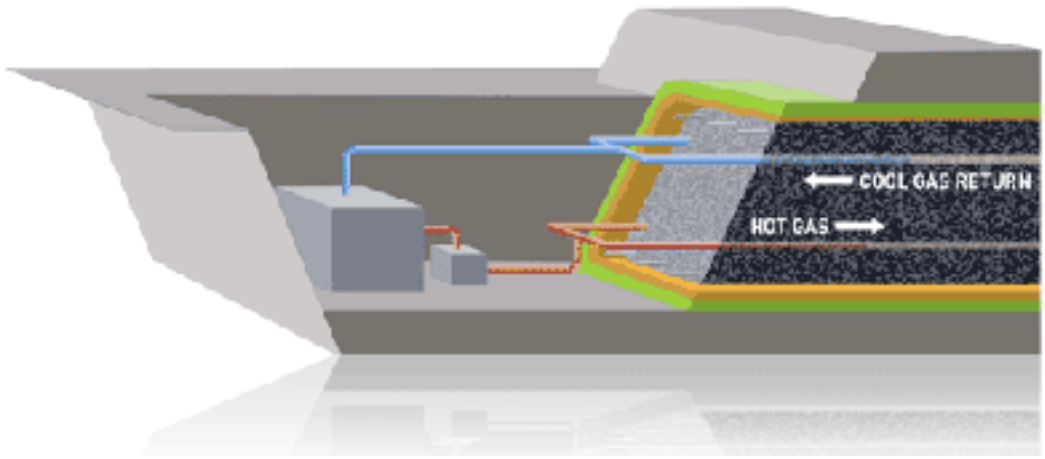

Figure 1. Schematic representation of Red Leaf Resources' EcoShale In-Capsule Technology.

To simulate the EcoShale capsule, a suite of software tools are needed in addition to STAR-CCM+. These commercial tools include EDEM, MATLAB, Gambit, and ICEM-CFD. EDEM is a computer-aided engineering (CAE) software platform employing discrete element method (DEM) technology. We use EDEM to generate representative oil shale particles inside the computational domain. Matlab is a computing environment and a programming language that we use to convert Star-CCM+ file format to a Gambit-readable file. Gambit is a CFD meshing package that is used to create a CFD-compatible geometric representation of the computational domain.. Gambit, however, is no longer commercially available and supported because the company has been acquired by ANSYS. However, the technology from Gambit has been implemented into a new geometry and meshing tool, ICEM-CFD, released by ANSYS.

In the early stages of creating the rubblized bed geometry, we used the commercial software EDEM to simulate the random shale distribution inside of the EcoShale capsule. However, during the course of this project, CD-adapco implemented a DEM solver into Star-CCM+. Therefore, we have shifted our geometry development efforts toward implementing the DEM capabilities present in Star-CCM+ to generate the random shale distribution geometry representing the EcoShale capsule.

Representative Computational Domain

In this section we define the representative domain and detail the geometry creation procedure necessary to approximate the rubblized pieces of oil shale inside that domain.. To resolve the convective heating channels between each of the pieces of shale as well as model each rubblized piece of shale, the representative domain is a subsection of the actual EcoShale capsule; this resolution for the entire EcoShale capsule was not computationally feasible. This subsection, shown in Figure 2, represents a middle segment of the EcoShale capsule with a statistical representation of the oil shale piece distribution..It is 8 feet wide, 8 feet deep, and 17 feet tall, and contains two heating pipes. The height of the domain, 17 feet, is the same as the actual EcoShale capsule, but the width is chosen so that the left edge of the representative computational domain is halfway between the current set of the heating pipes and the neighboring set of heating pipes on the left hand side. The same applies for the position of the right side of the representative computation domain. The depth is chosen to be the same as the width. Therefore, the representative computational domain captures a repeating section of the EcoShale capsule in both the front-to-back as well as side-to-side directions.

During the initial stages of this project, rather than using the full representative geometry (Figure 2) to determine simulation procedures and numerical settings, we have defined a reduced size representative geometry shown in Figure 3. The dimensions of this reduced size computational domain are 5 feet by 5 feet by 5 feet This reduced size representative computational domain provided faster turn around times for the simulations, thus allowing us to test and fine-tune a greater number of parameters, settings, and procedures.

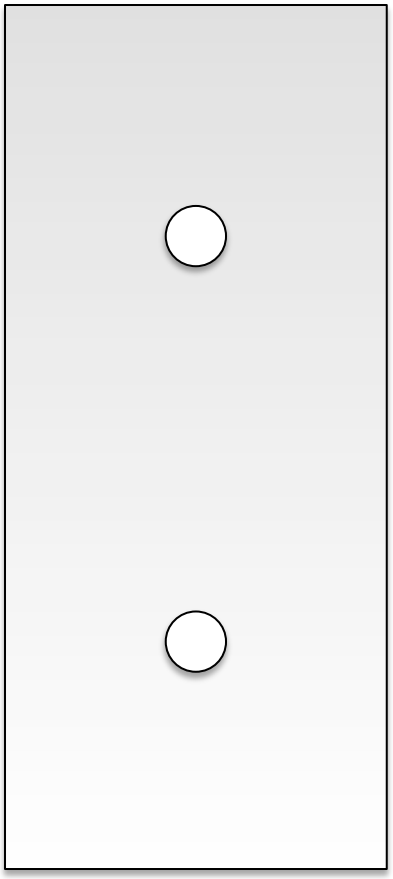

Figure 2. Front view of the full representative computational domain.

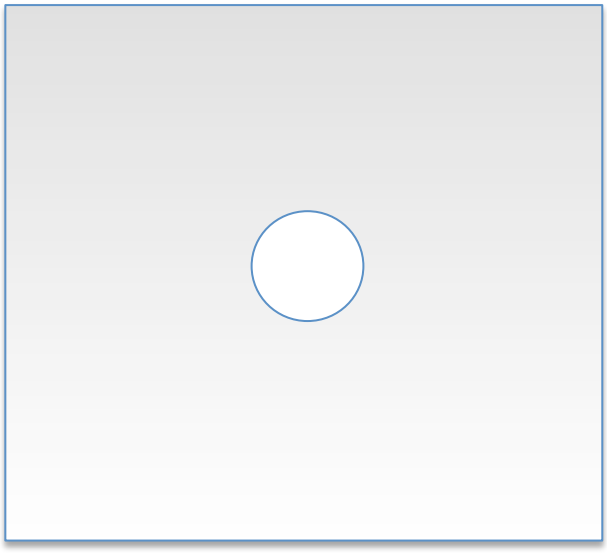

Figure 3. Front view of the reduced size representative computational domain.

CONSTRUCTION OF REPRESENTATIVE OIL SHALE PARTICLES

Discrete Element Method Simulation

To create a CFD simulation that contains both the fluid inside the convective channels as well as the solid particles representing each piece of shale, we first run a DEM simulation inside the Star-CCM+ package. In the DEM simulation, each shale particle is approximated by a grouping of spheres. The grouping of spheres may contain as few as one sphere or as many as multiple dozens of spheres in various shapes. Two such representative sphere groups for two pieces of rubblized shale are shown in Figure 4. For the DEM simulations, the smallest rubblized shale dimension is 0.5 feet and the largest dimension is 2 feet based on observations of particle size at the Red Leaf site. For most of the DEM simulations we have used cube-like particles with equal side lengths while still not exceeding the dimensions specified by Red Leaf.

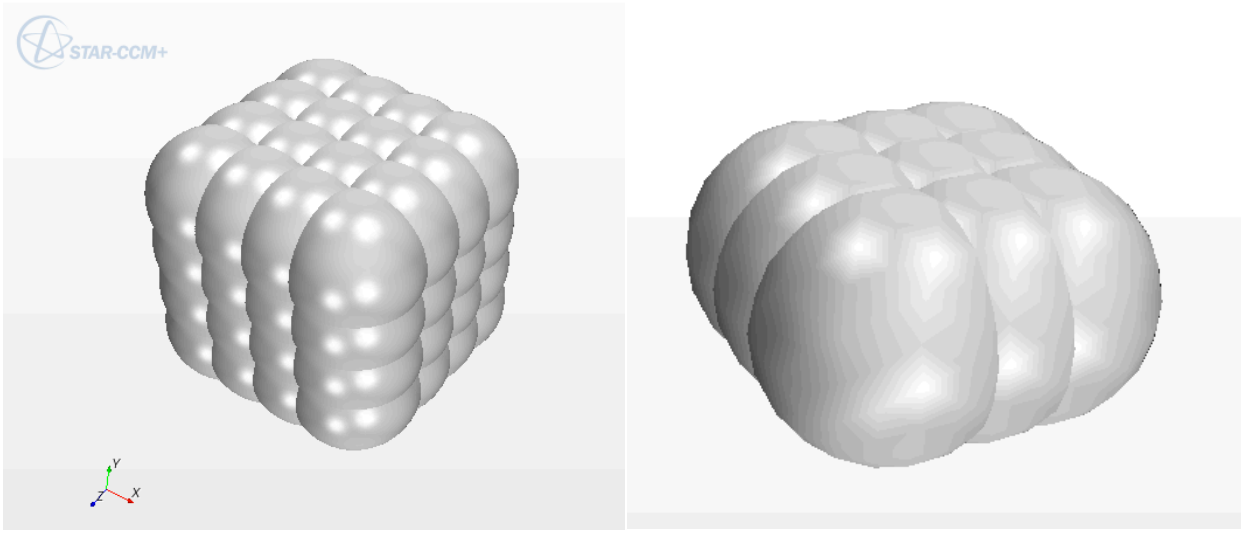

Figure 4. Two different shale particle approximations possible inside the Star-CCM+ DEM solver

Figure 5 shows a screen shot of the Star-CCM+ interface with the DEM simulation in progress for the full representative computational domain. To capture the statistical distribution as well as random orientation of oil shale particles inside the representative domain, the particles are introduced with random orientation and location at the top boundary of the computational domain and then allowed to fall and fill up the computational domain. The result of the DEM simulation is a domain packed with groupings of spherical particles. We use the same methodology to fill up the reduced size computational domain.

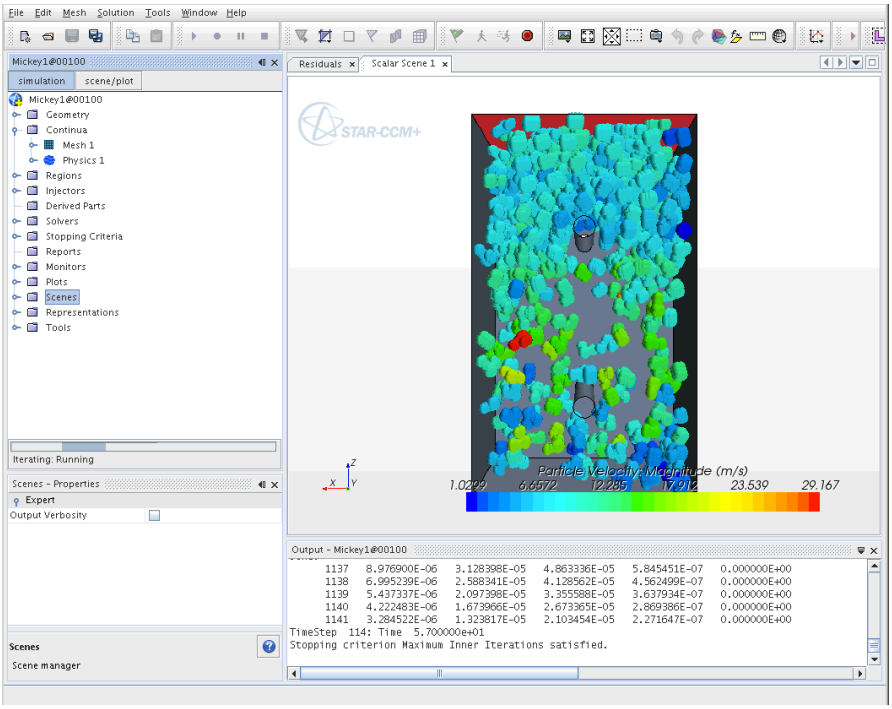

Figure 5. Screen shot of the Star-CCM+ user interface with DEM simulation in progress.

Processing DEM Simulation Results

We export the DEM simulation results (i.e. representative domain packed with groups of spheres) into a .csv (comma separated value) file, which contains the information regarding the center and radius of each sphere as well as how many spheres are in one grouping. Since this information is exported for each grouping of spheres, we can process the information using MATLAB and create an actual geometric representation of the rubblized pieces of oil shale inside Gambit meshing software. The processing step in MATLAB allows us to fine tune our geometric representation of each oil shale particle – we can either leave the shale particle with rounded edges (see Figure 4) or we can create an *envelope* for each grouping of spheres and transform the grouping into a cuboid particle. The graphical representation of this process is shown in Figure 6. Figure 7 shows the DEM results (sphere groupings) converted into cuboid particles using the MATLAB code and imported into Gambit.

This final representative shale geometry, whether rounded or cuboid, is then exported back to Star-CCM+, where, after setting up the appropriate boundary conditions and solution settings, the CFD simulation is completed. This streamlined process for geometry creation allows us to side-step the memory limitations that occur when the DEM simulation results are processed directly in Star-CCM+.

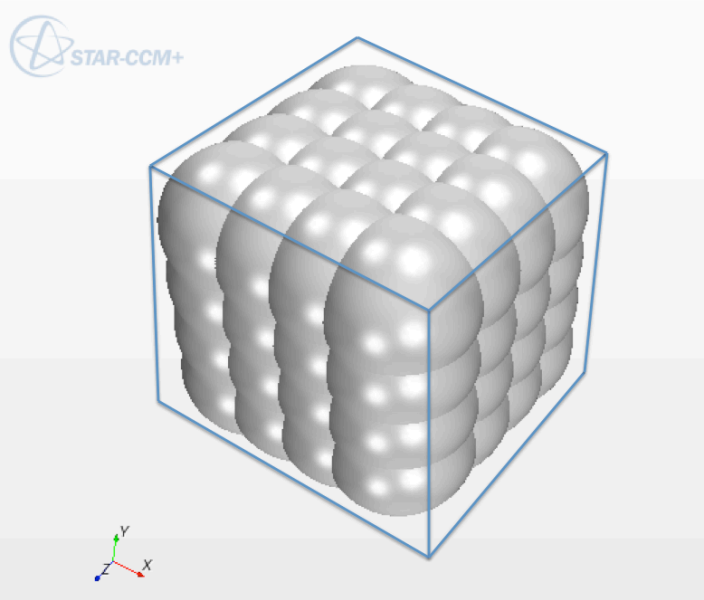

Figure 6. Illustration of a sphere particle grouping being converted to a cuboid representation oil shale particle using MATLAB programming language.

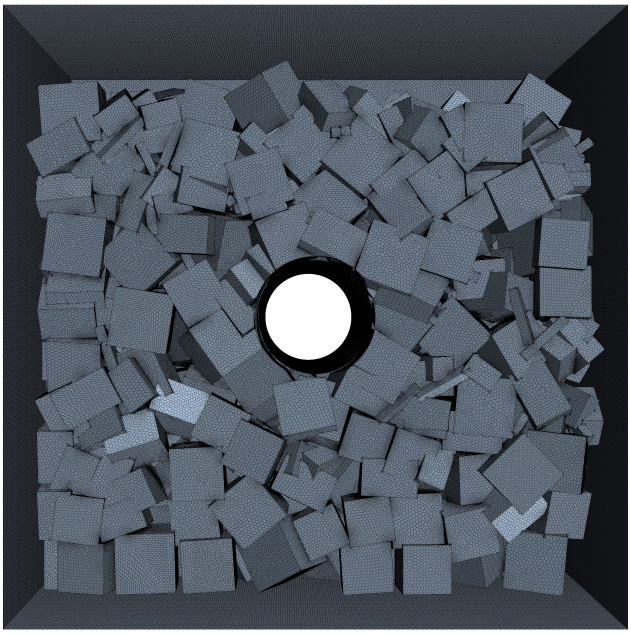

Figure 7. Reduced size representative computational domain filled with cuboid particles representing pieces of shale.

New DEM Processing Software Tools

For all of the geometric representations of oil shale presented in this report, whether round or cuboid, we rely on Gambit meshing software for converting DEM simulation results into geometric representations of oil shale. However, Gambit software tool is no longer commercially available. Therefore, we have explored new possibilities and software packages to replace Gambit. One package that we are currently evaluating is ICEM-CFD, a new geometry and meshing tool developed by ANSYS. It is commercially available and offers support. A sample of the oil shale particle geometry creation process inside ICEM-CFD is shown in Figure 8. In the future, we plan to evaluate more software tools that would allow us to accomplish our goal of creating an approximation to the shale particles inside our representative geometric domain.

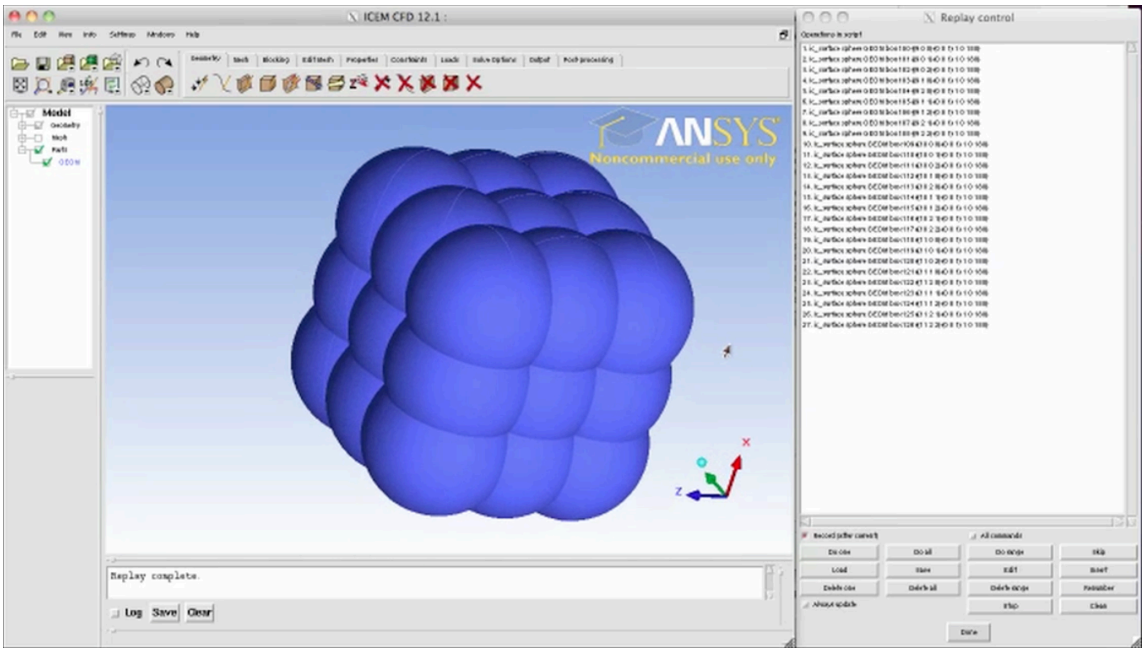

Figure 8. Sample particle generated in the new meshing and geometry software ICEM-CFD.

COMPUTATIONAL FLUID AND SOLID SIMULATIONS

In order to create a CFD-based simulation tool that can be used for validation studies, our computational efforts were divided into three main tasks: 1) to model heat transfer in the fluid region of the computational domain, including flow around obstacles, 2) to establish capability to model heat transfer inside the solid regions representing the pieces of rubblized shale, and 3) to couple the simulation of both the fluid and solid regions into one computation.

Initial Fluid-Only Simulation

For the initial simulation, designed to show the capability of Star-CCM+ to capture buoyant heat flows, we used the reduced size computational domain shown in Figure 3 and performed an unsteady simulation with the Reynolds-Averaged Navier-Stokes (RANS) turbulence model. For the pipe boundary condition, we used the same heating temperature used by Red Leaf in their pilot-scale EcoShale capsule. We assumed the rest of the domain was at normal air temperature and that the boundaries were insulated. The velocity distribution for this simplified case is shown in Figure 9 and the temperature distribution is shown in Figure 10. As can be seen from these figures, the simulation did capture the buoyant heat rising from the pipe until it reached the top boundary. The heat then accumulated in the upper part of the domain and started to heat the rest of the domain from the top down. This behavior is the result of the hot convective currents that we aim to resolve and simulate in our representative domain with a statistical distribution of oil shale pieces.

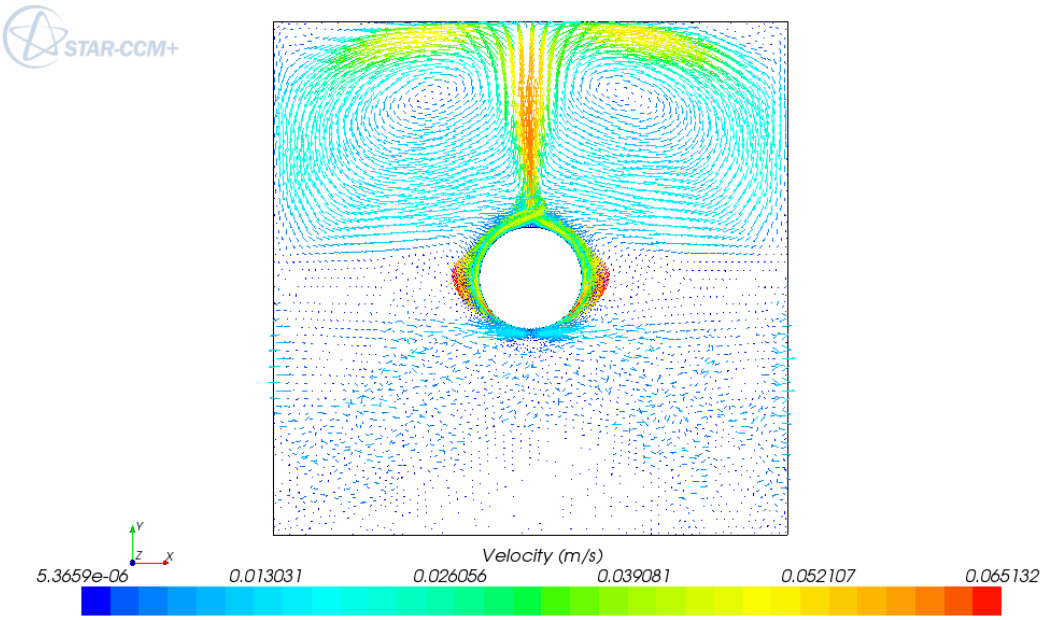

Figure 9. Front view of the velocity field distribution for the fluid-only simulation inside the reduced size computational domain with no shale particles.

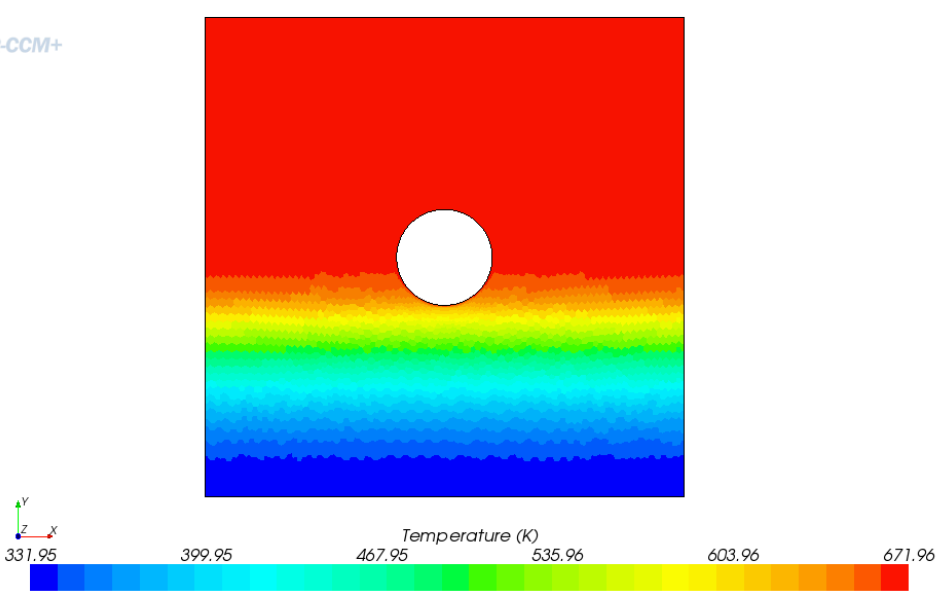

Figure 10. Front view of the temperature distribution for the fluid-only simulation.

Fluid-Only Simulation of Eight-Piece Shale Domain

Our subsequent simulation was designed to test the geometry creation technique, starting with the DEM simulation, converting those results (i.e. geometry representations) to a Gambit geometry, which was subsequently converted and imported back to Star-CCM+. The geometry, shown in Figure 11, contains eight pieces of shale. Each cubic shale particle shown in Figure 11 was created by applying the MATLAB script on the sphere groupings from the DEM simulation. While this computational geometry is extremely simplified, it was useful for evaluating geometry creation strategies, testing the sensitivity of boundary conditions, and providing a starting point in creating more complex geometries and simulations.

We have used the geometry shown in Figure 11 to run a suite of simulations. These simulations are used to 1) evaluate the meshing schemes used for the fluid part of the domain only, and 2) to test the effect and sensitivity of thermal boundary conditions used in the simulation on the heat distribution inside the computational domain.

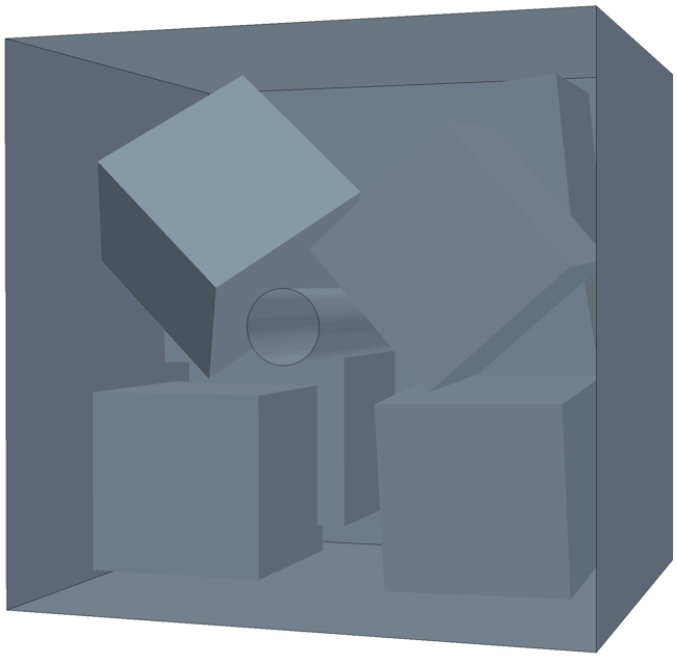

Figure 11. Eight-piece oil shale geometry in a reduced size representative computational domain.

Meshing Techniques

For this simulation, an LES model is used. LES models are able to resolve the unsteady vortex structures and turbulent eddies of the hot gases rising through the representative domain with greater detail than the RANS models. Since we expect these vortex structures to influence and to contribute to the convective heat transfer between the fluid and the solid particles, an LES turbulence models is more appropriate for this simulation.

Our initial simulations yielded the temperature distribution shown in Figure 12 and the velocity vectors colored by velocity magnitude shown in Figure 13 with blue color representing the low velocities and the red color representing the high velocities. Even though temperature distribution seems physical (i.e. the hotter fluid is located in the upper part of the domain and the cooler air is in the lower part), the solution residuals were exceptionally high. Using post-processing techniques, we linked these unusually high residuals to the velocity fluctuations in two problematic regions: 1) the computational cells near the corner areas of the shale pieces and 2) the narrow spaces between two neighboring pieces of shale. These two regions are characterized by highly skewed computational cells of the fluid mesh. Therefore, we have considered the following two meshing strategies available in Star-CCM+: 1) eliminating the problematic corner areas by using the surface-wrapping meshing model, and 2) preserving the sharp geometric features by further refining the mesh.

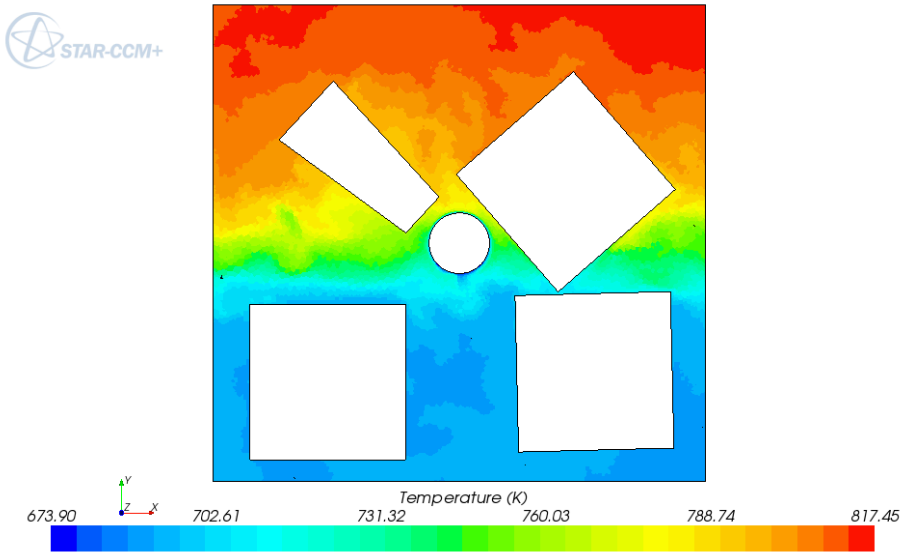

Figure 12. Temperature distribution in the fluid region of the eight-piece shale domain.

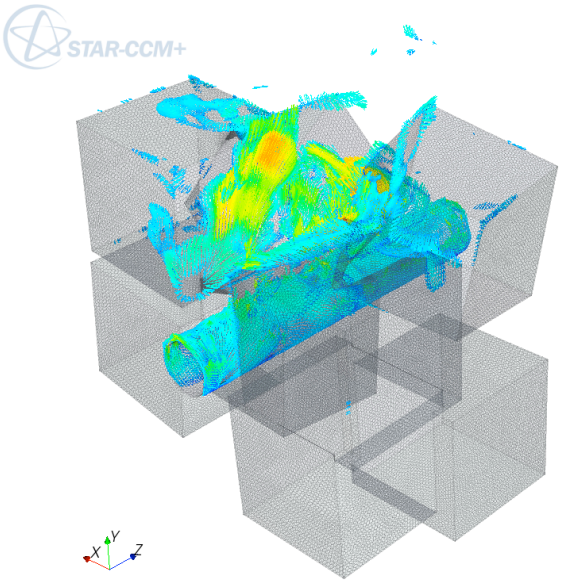

Figure 13. Velocity vector representations for the eight-piece shale domain colored by velocity magnitude.

Surface wrapping is generally used to wrap problematic details in the geometry such as the corner of a cube or a sharp angle between two pieces of shale. Surface wrapping corrects the sharp areas of the geometry or eliminates difficult areas by combining regions. Figure 14 shows a comparison of the previous geometry details in the eight-piece shale computational domain to the wrapped surface geometry. As can be seen from Figure 14, the corner of a cube is merged into the cube below it, which increases contact angles and eliminates the problematic area. However, this model creates new difficulties in preserving independent pieces of oil shale.

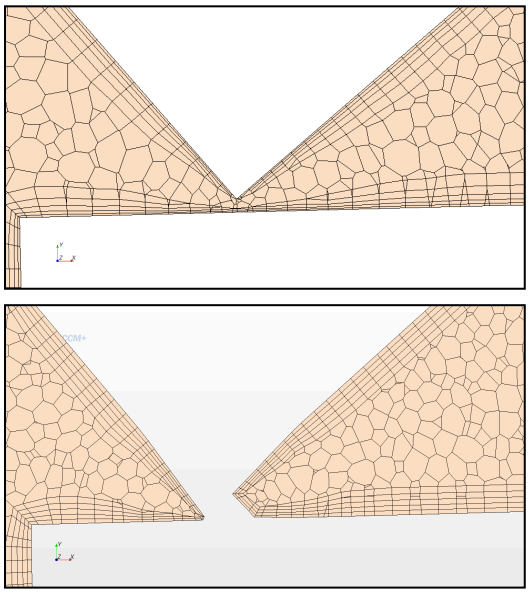

Figure 14. Comparison of original geometry and mesh (top) with the newly-adapted wrapped surface geometry and mesh (bottom). In both graphics, the white region represents the oil shale particles and the mesh shows the fluid portion of the computational domain.

The mesh refining strategy preserves the complex geometrical features by decreasing the computational cell size. Figure 15 and Figure 16 show images of the refined mesh that eliminates the highly skewed cells. Using this refined mesh eliminates the solution fluctuations seen in the simulation with a coarser mesh representation. However, the number of cells in this mesh is excessive, thus greatly increasing the computational time required to obtain a converged solution. Additionally, neither of these methods address a second vexing problem that occurs in the more complex geometric representations of the rubblized oil shale: that of the presence of internal gas volumes trapped among multiple pieces of shale. These regions create independent flow domains that cannot be solved simultaneously with the open flow channels and cause the simulations to diverge almost immediately.

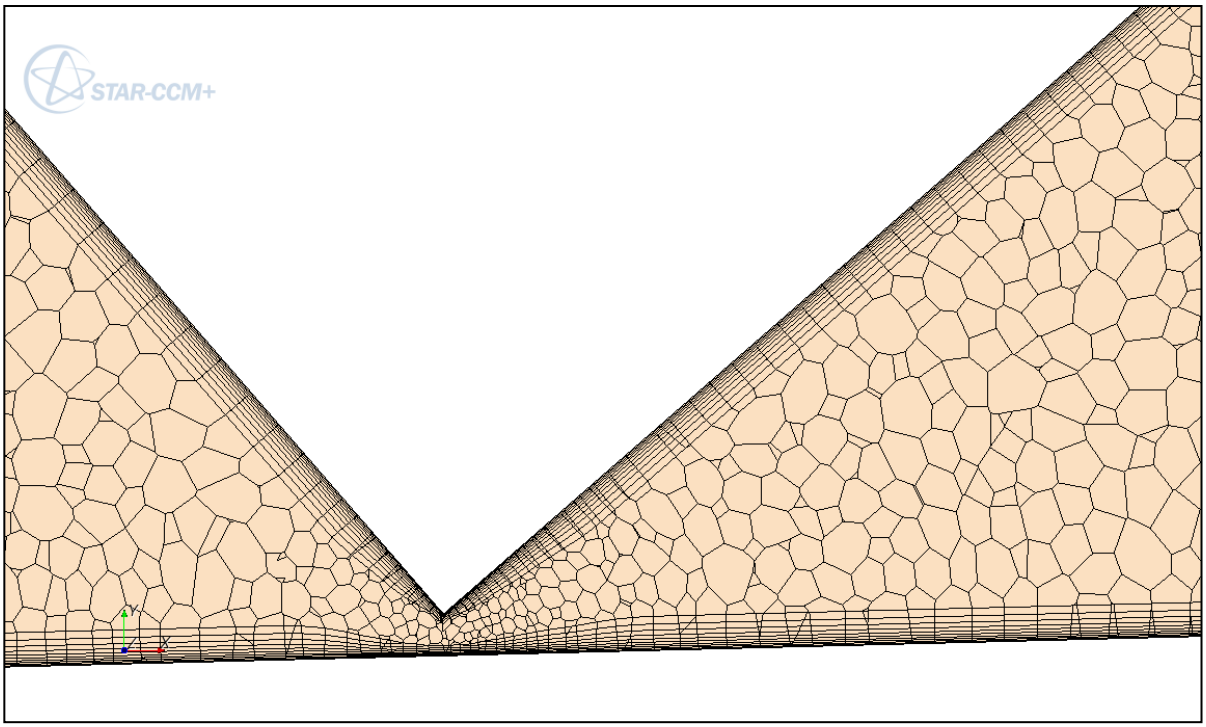

Figure 15. Refined mesh – close up view of problematic area.

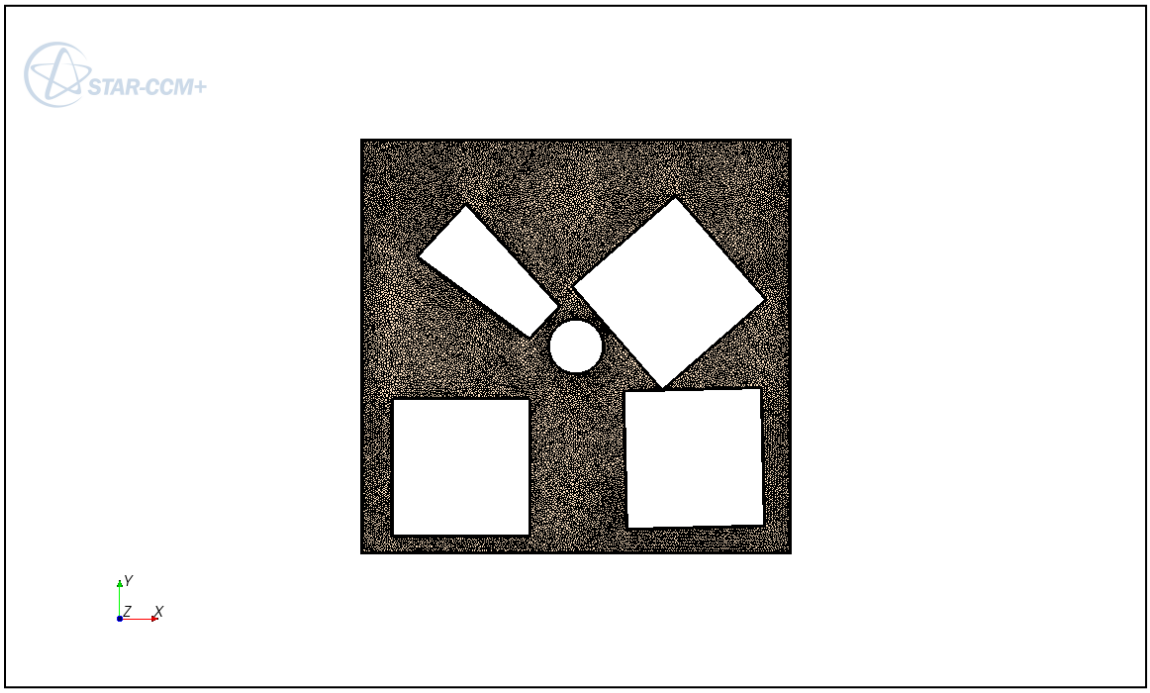

Figure 16. Refined mesh – view of a plane through the computational domain.

Boundary Conditions Sensitivity Study

The next step was to consider the effects of boundary conditions on the simulation results. Because of the large computational cost associated with simulations that include the extended domain and the two solid phases, fluid and solid, boundary condition sensitivity tests were conducted using the computational domain shown in Figure 11 and only considering the fluid phase. The simulation was performed on a polyhedral mesh with around 14 million elements in the fluid region (the fine computational mesh described in the previous section). An implicit laminar solver with a time step of one second was used. Because of the fine resolution and time step used to advance to solution, we switched from the LES model to the laminar model, which, in essence, represents the Direct Numerical Simulation (DNS) model.

For the study of simulation sensitivity to the boundary conditions, we have considered the following three scenarios: 1) adiabatic (perfectly insulated) boundaries for both the geometry domain as well as pieces of shale, 2) adiabatic boundaries at the geometry edges and a constant temperature (300 K) boundary condition for the pieces of shale, and 3) constant temperature (300 K) boundaries for both the geometry edges and the pieces of shale. The constant temperature boundary condition for the geometry domain in the last scenario represents a poorly insulated system. Furthermore, the constant temperature boundaries for the shale pieces are based on the vastly different heating time scales for the fluid and solid regions – because of the thermal conductivity properties, the fluid heat up time is much shorter than the solid phase heat up time. Because of this time scale difference, we can study the effect of boundary conditions on the fluid phase only and eliminate the complexity introduced by modeling the solid phase as well. Because of the short simulation times, the temperature increase in the pieces of shale is assumed to be negligible in comparison to the temperature increase in the fluid region. This assumption reduces the computational cost of the simulations by omitting the simulation of solid heat transfer. Thus, these three scenarios span the possible extremes in boundary conditions expected for such a system in reality.

Thermal profiles inside the computational domain for the three scenarios described are shown in Figure 17, Figure 18, and Figure 19, respectively. These figures show two perpendicular planes: the right plane shows temperature distribution inside the computational domain, and the left plane shows the velocity distribution. In all figures, the white space represents the shale particles, which were not considered for these simulations. All three profiles are shown at the same simulation time of 8,861 seconds. It is clear from a comparison of the figures that the thermal profile inside the test bed is very sensitive to the boundary conditions. The greatest temperature increase is seen in the perfectly insulated system (Figure 17), while the smallest temperature increase is seen in the non-insulated system (Figure 19). The most realistic scenario with mixed boundary conditions (Figure 18) shows a temperature distribution between the

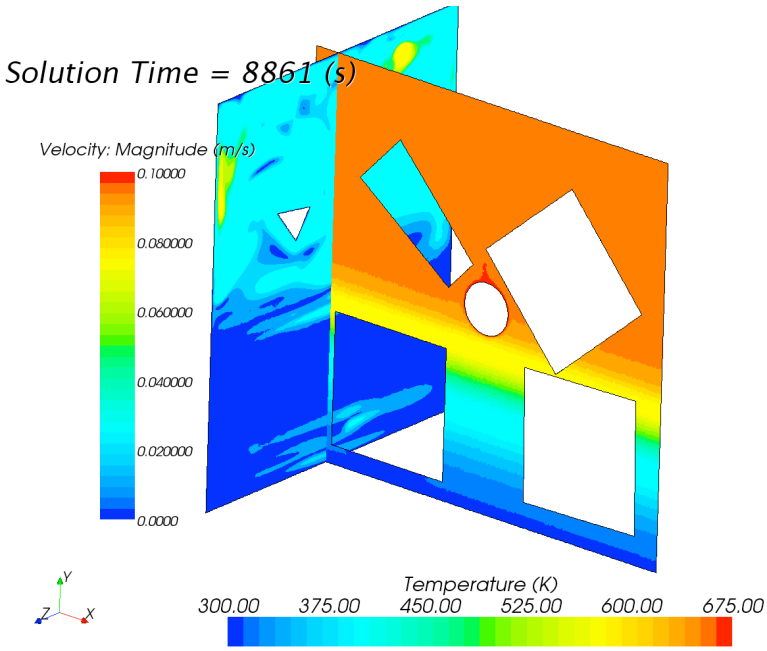

Figure 17. Temperature distribution inside a perfectly insulated domain.

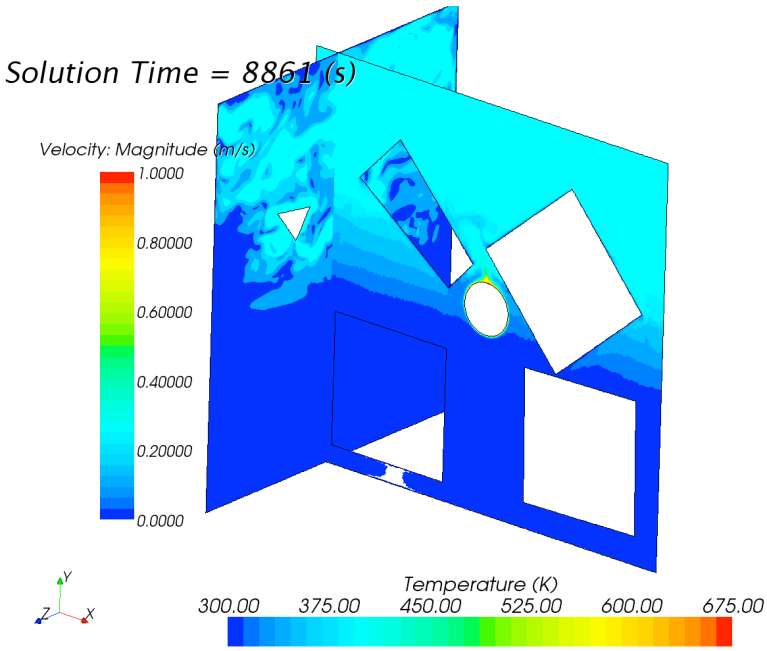

Figure 18. Temperature distribution inside a domain with perfectly insulated external boundaries, and pieces of shale fixed at constant temperature of 300 K.

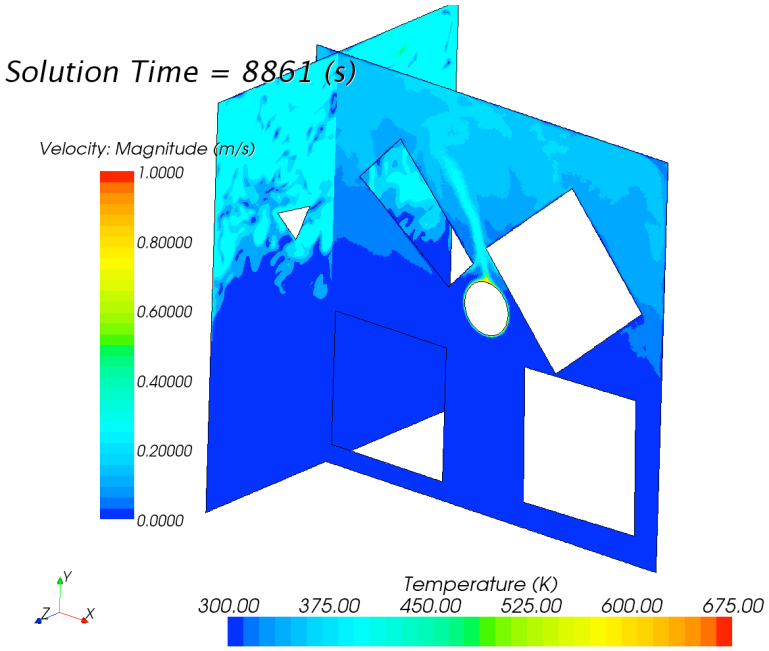

Figure 19. Temperature distribution inside a representative non-insulated domain with external boundaries and pieces of shale at a constant temperature of 300 K.

insulated and non-insulated systems. Based on these results, it is very important to: 1) insulate the experimental system extremely well to reduce heat losses and to increase the available heat to the pieces of shale, and 2) have an accurate description of the experimental boundary conditions. Without knowing the exact boundary conditions used in the experiment, consistency between the experimental and simulation temperature distributions will be difficult to obtain.

To understand the time evolution of the temperature field inside the test bed, we once again used the computational domain shown in Figure 11 with the boundary conditions of the second scenario described above - perfectly insulated domain boundaries and pieces of shale set at a constant temperature of 300 K. The simulation results are shown as two perpendicular planes in Figure 20: the right plane shows the temperature distribution inside the computational domain at the labeled time, and the left plane shows the velocity distribution within the computational domain at the same time. As can be seen from this figure, the greatest heating occurs in the first 1,000 seconds of the simulation, after which the overall heating rate inside the test bed decreases considerably. The initial heating is caused by the buoyant mixing of the hot air supplied by the heating element that rises through the convective channels between the pieces of shale. As the air temperature above the heating element increases, the buoyancy effect is reduced; heating progresses from the upper part of the domain to the lower part of the domain at a substantially reduced rate. Most of the subsequent heat transfer occurs through conduction. Based on these

simulation results, we can conclude that the best placement for the heating element is close to the bottom of the test bed. Such a placement would allow for more effective buoyancy-driven mixing inside the test bed, thereby increasing the overall temperature inside the shale bed more rapidly.

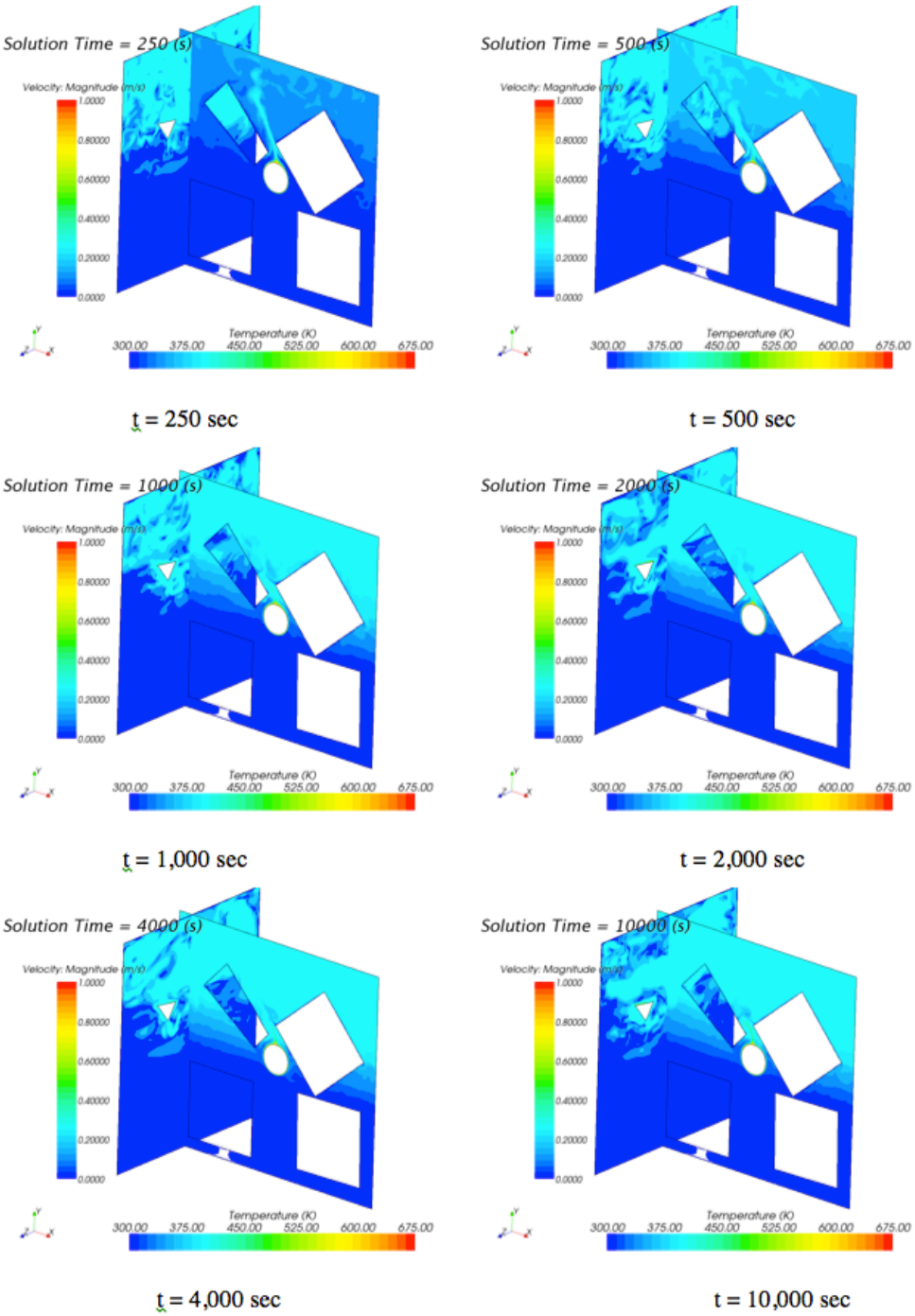

Figure 20. Time evolution of a thermal profile inside the simplified computational domain.

New Simulation Methodologies

To address the challenges described in "Meshing Techniques," we have developed a two-pronged strategy. First, we circumvented the meshing problems by simplifying the shale geometry, e.g. shale geometry with rounded edges as shown in Figure 4, allowing us to rapidly complete a full heat-transfer coupled simulation. This modification of the geometrical representation of the pieces of rubblized shale presents two main advantages: 1) it helps to preserve the particle local coordinate system, which is important for implementation of directional properties of the oil shale, and 2) it produces smooth edges for an even more improved computational mesh. Second, we retained the cuboid representation of shale particles as shown in Figure 7 and continued to explore methods for resolving the outlined meshing difficulties. This two-pronged strategy yielded a higher probability of meeting the needs of our industrial partner, Red Leaf Resources, in a shorter time period.

The strategy for rapid prototyping of the overall simulation process involved using tools available in the latest version of Star-CCM+ software, namely the newly implemented DEM model, and using the MATLAB script to convert the sphere groupings from the DEM simulation to rounded particles. This tool allowed us to produce the rounded shale particles, as shown in Figure 4, thereby omitting the significant difficulties encountered in 1) creating a mesh with the surface wrapping model or 2) decreasing the computational cell size by refining the mesh.

To demonstrate the new Star-CCM+ DEM capabilities, we created a sixty-two particle oil shale geometry (which corresponds to sixty-two sphere groupings) inside the reduced-size computational domain shown in Figure 3. All the particles were uniform in size, about 0.5 feet per side. After exporting the DEM results to Gambit and subsequently importing the geometric shale representation back to Star-CCM+, we meshed the resulting domain using the surface wrapping model and a polyhedral volume mesh with a total of 3.5 million cells. This geometric representation is shown in Figure 21. Because of the rounded edges on each particle, meshing was a straightforward process; no extra time was required to produce an improved simulation mesh. Unfortunately, this rapid prototyping with DEM does not allow for a realistic oil shale representation because of the rounded edges (in comparison to the sharp, jagged edges present in the actual EcoShale capsule) and the same-sized oil shale particles (in comparison to the varying shale size inside the EcoShale capsule). The work of improving the geometric representation of the rubblized oil shale capsule so that it better resembles the EcoShale capsule geometry will continue into Phase II of this project.

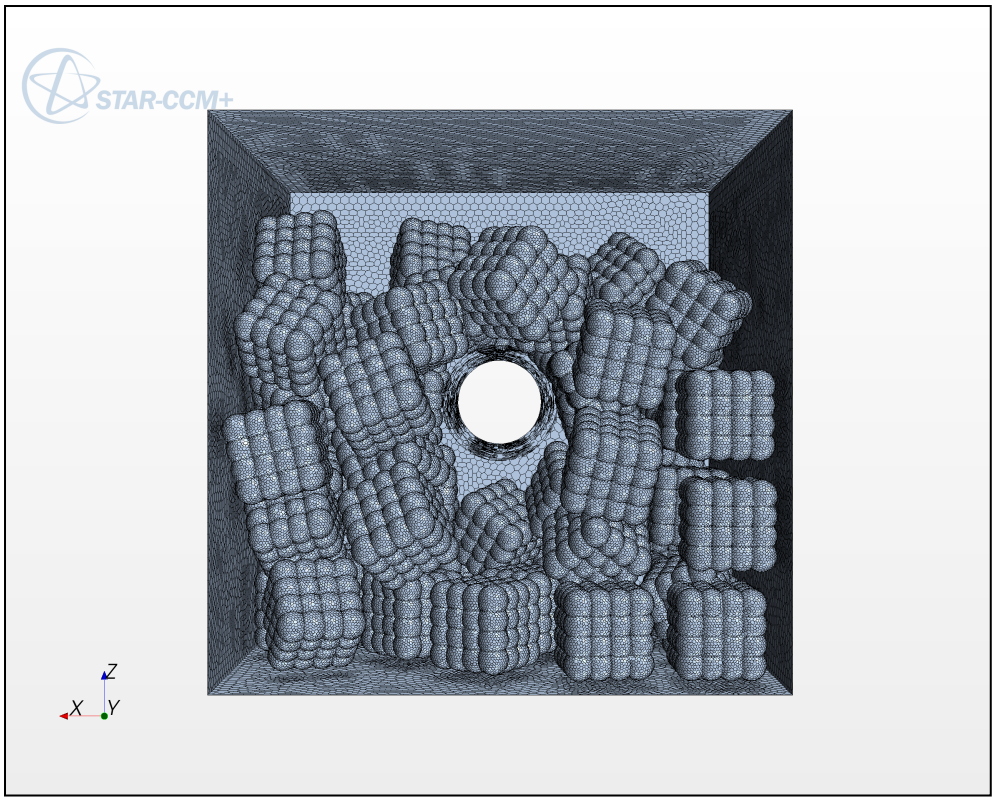

Figure 21. Reduced-size domain representation with sixty-two shale particles.

Fully transient flow simulations on the geometry shown in Figure 21 were performed with heat transfer to both the fluid and solid phases; fluid flow settings were the same as described in the "Boundary Conditions Sensitivity Study" section. All outside boundaries of the domain were set to adiabatic boundary condition (perfectly insulated), whereas an interface boundary condition was used for the shale pieces. The interface boundary condition allows for the conductive heat transfer between the fluid and solid phases. Figure 22 and Figure 23 show the velocity vectors and the temperature field, respectively, in a front-view slice through the computational domain after 22.5 minutes of simulation time. A buoyant plume of hot air can be seen rising through the domain and interacting with the pieces of shale; the pieces of shale in the pathway of the plume are heated by the convective current.

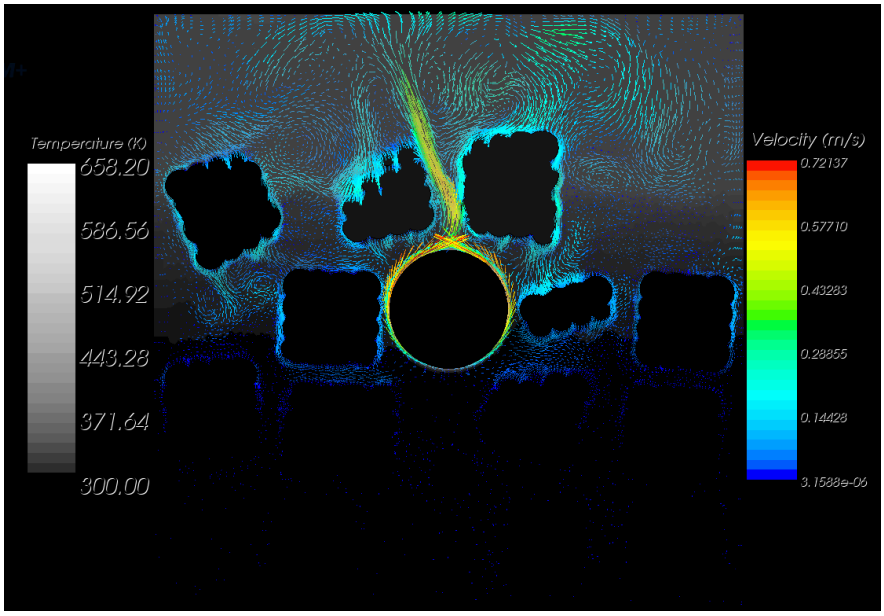

Figure 22. Velocity vectors in a plane inside the domain for the laminar simulation.

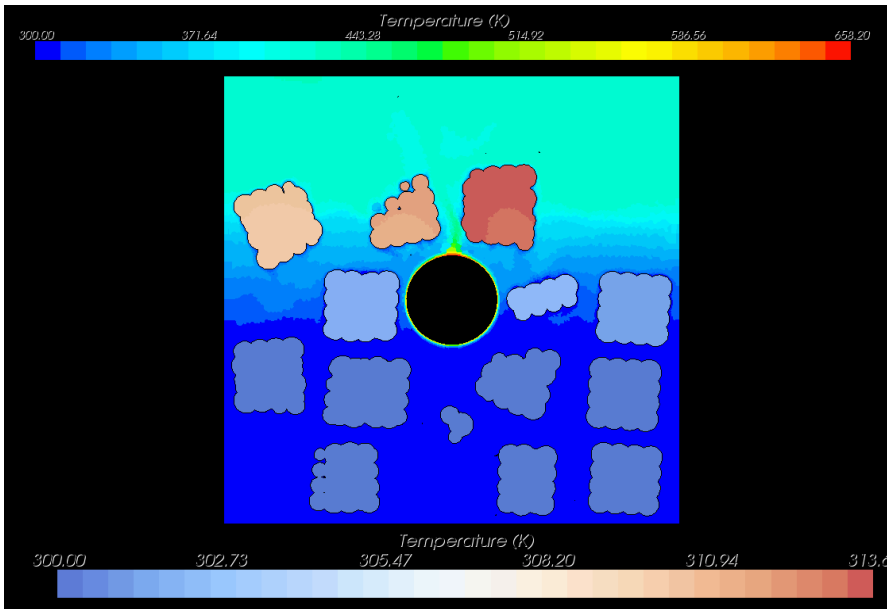

Figure 23. Temperature profile in both oil shale and fluid regions in a plane inside of the computational domain for the laminar simulation.

Next, we increased the complexity of the simulation by using the full representative domain shown in Figure 2 in order to test the ability of Star-CCM+ to generate and handle larger quantities of particles. The full domain features two heating elements and contains about 2,000 pieces of shale as shown in Figure 24. Each piece of shale is created from a group of 27 spheres, not from a grouping of 64 spheres as in previous simulations. This change reduced the computational cost of the DEM simulations, thus avoiding memory usage issues associated with

a larger number of pieces of shale. The computational mesh, including both fluid and solid phases, contained 8.4 million polyhedral cells. Once again, the unsteady laminar implicit solver with time step size of 0.1 seconds was employed for the fluid phase.

Figure 24. Full size representative computational domain containing about 2,000 oil shale pieces.

The computational cost associated with simulations involving heat transfer in both fluid and solid phases is high; the simulation was run on 612 processors, with one minute of simulation time corresponding to about 300 minutes of actual time. Figure 25, Figure 26, and Figure 27 show the coupled fluid/solid simulation results for the extended domain. Figure 25 and Figure 26 are taken at 418 time steps into the simulation and show the velocity vectors and the temperature profile for a plane in the middle of the computational domain, respectively. Buoyant velocities are approaching 1.5 m/s inside the convective channels. The upward buoyant plume of hot air interacts with the oil shale particles and mixes throughout the computational domain.

Figure 27 is taken after 974 times steps. In this figure, the pieces of shale located in the direct pathway of the hot air convective current show the largest temperature change. Also of interest in Figure 27 are the vastly different heating time scales for the fluid and solid regions. In the upper region of the domain, the fluid temperature increased by approximately 100 K from the initial condition while the temperature of shale in the same region increased by only 2-4 K.

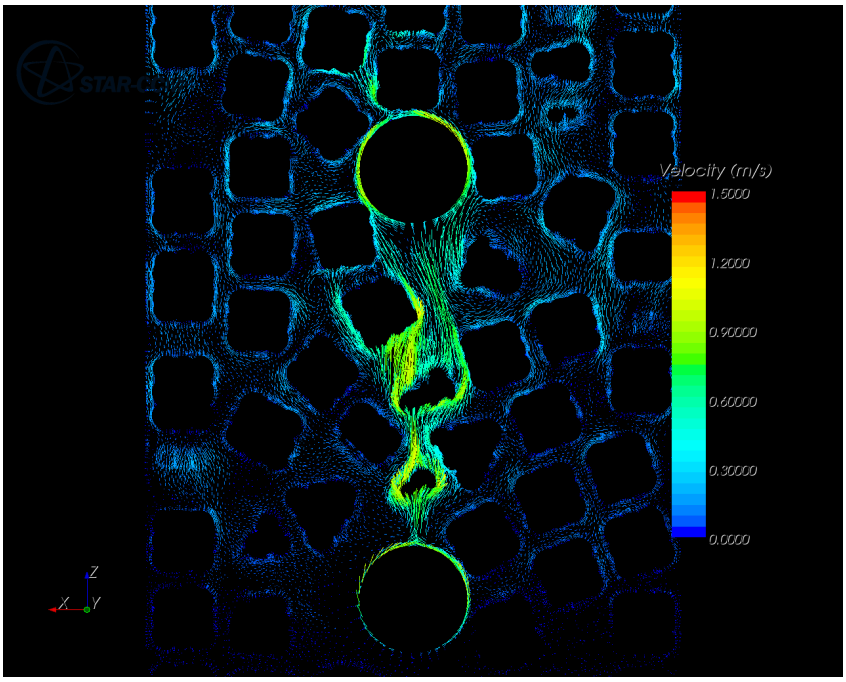

Figure 25. Front view of the velocity vectors for the full size computational domain simulation in a plane inside of the domain.

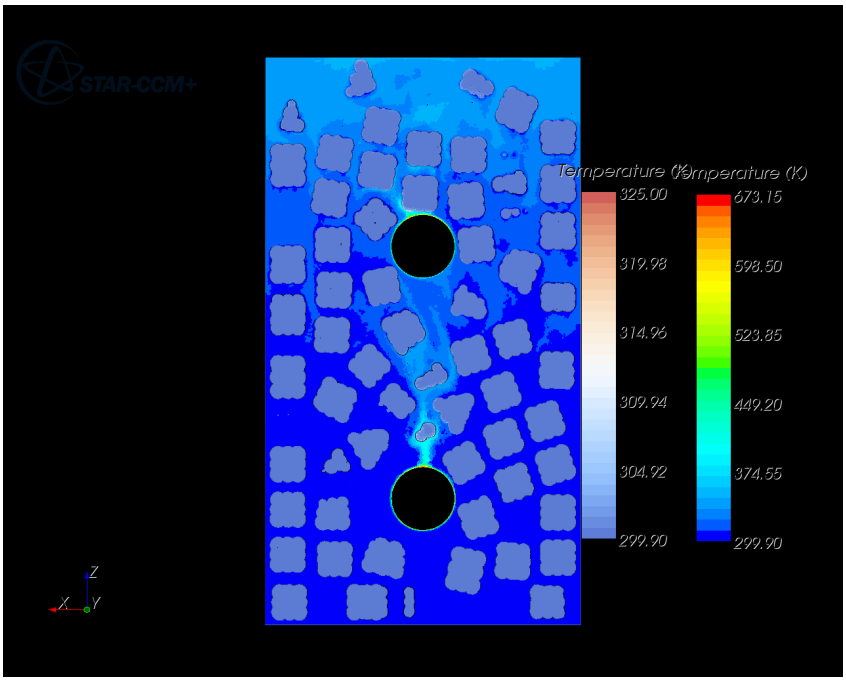

Figure 26. Temperature profile in both solid and fluid phases for the full size computational domain simulation.

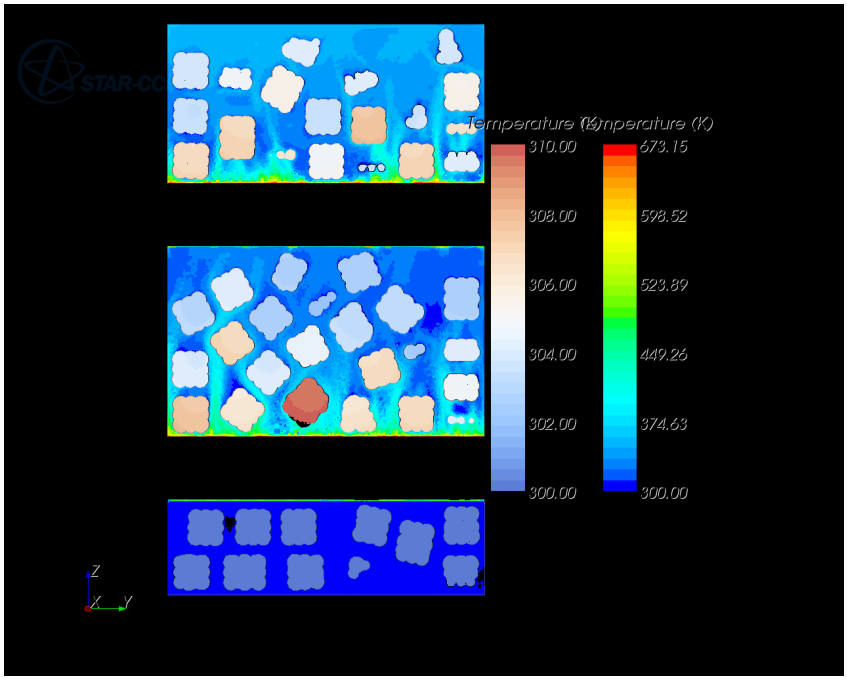

Figure 27. Side view of the temperature profile in the fluid as well as solid (shale) regions in plane inside the full size computational domain simulation.

Operator-Splitting Numerical Procedure

Because the conductive and convective heating time scales are of different magnitudes, as illustrated in Figure 27, the simulation of heating throughout the entire domain using conventional solution algorithms requires very large computational resources. To address this issue, we have modified our solution algorithm to include an operator-splitting procedure. This solution technique allows us to efficiently simulate the long-term thermal effects occurring inside the rubblized oil shale bed geometry. This algorithm implementation represents a significant step forward in obtaining the temperature history of oil shale particles on the order of days and weeks instead of minutes while using the same amount of computational resources.

This algorithm takes advantage of the difference in the magnitude of time scales present in our problem. The fluid *convective* time scales are much shorter than the fluid and solid *conductive* thermal time scales. Hence, once the simulation achieves a statistically steady state, effects of the faster convective fluid currents decrease and the slower thermal conductive effects, present in both fluid and solid phases, dominate.

Up until this point, we have employed the traditional iterative solution algorithm shown in Figure 28. The solution for both smaller and larger times scales is advanced concurrently, thus restricting the maximum allowable time step required for the simulation to remain stable. For each time step, the fluid continuity and momentum equations are solved first, followed by the solution of the fluid and solid energy equations. Only then is the time step advanced.

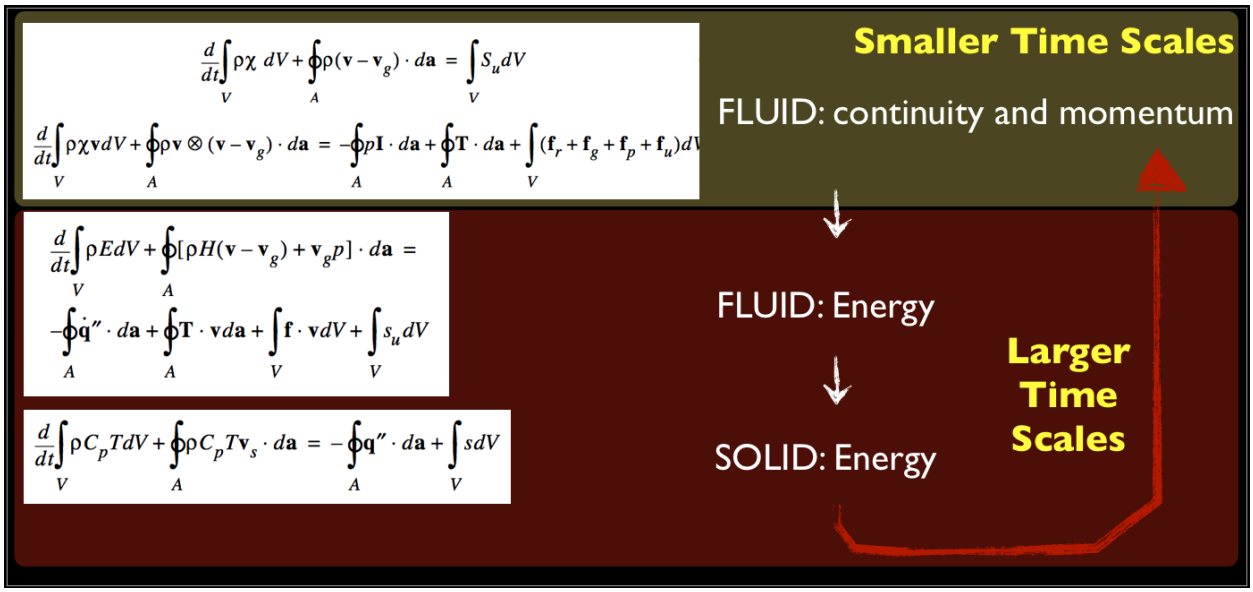

Figure 28. Traditional iterative solution algorithm for fluid convective currents and for fluid and solid thermal solutions.

The modified solution algorithm, Figure 29, is subdivided into two sections: 1) the traditional solution algorithm is employed to advance the fluid continuity and momentum equations along with the fluid and solid energy equations concurrently until a statistically steady fluid flow and thermal solution is obtained, 2) the time-intensive computation of fluid continuity and momentum is disabled and only the fluid and solid energy equations are solved, a process which allows us to increase the numerically-stable simulation time step from seconds to multiple minutes, thereby significantly increasing the computational speed. After about one hundred large time steps, the simulation is reverted back to the traditional algorithm for a few time steps to allow the fluid flow field solution to adjust based on the new temperature gradients. Once a statistically steady state solution is achieved, the simulation reverts back to solving only the fluid and solid energy equations while omitting the fluid continuity and momentum equations. This solution strategy can be repeated iteratively until a converged thermal distribution inside the rubblized oil shale bed is obtained.

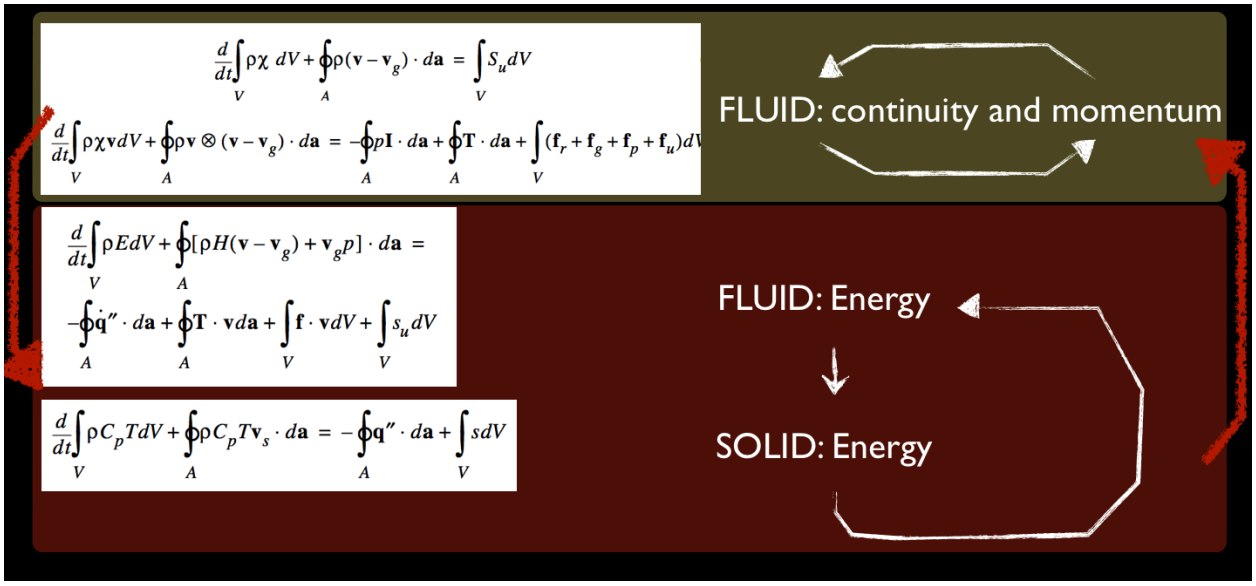

Figure 29. Modified solution algorithm with operator splitting used to separate the solution for time scales of differing magnitudes.

Simulation results obtained at solution times of 0.5 seconds, 83 seconds, 183 seconds, 14,998.5 seconds, and 112,500 seconds using the newly developed operator-splitting algorithm are shown in Figure 30. For the first 83 seconds, the traditional iterative solution algorithm is used to advance the solution at a time step of 0.5 seconds to initialize both the convective and thermal fields. After 83 seconds, only the solution for the fluid and solid energy equations is advanced at a time step of 100 seconds. After 14,900 seconds, the simulation time step is decreased to 0.5 seconds and all continuity, momentum, and energy equations are solved until a statistically steady state solution is achieved. At simulation time of 14,900 seconds, we once again stop iterating the fluid continuity and momentum equations and only solve the energy equations with a time step of 500 seconds. The solution is then advanced to 112,500 seconds (31 hours of simulation time). Even when using a time step of 500 seconds, the large conductive thermal scales that occur within the computational domain are resolved, thus capturing the heat transfer within the fluid as well as the heat transfer between the fluid and solid particles. With this solution algorithm, we observe a significant increase in temperature of the oil shale particles. With the traditional algorithm, it would not have been possible to advance the simulation to this point without using excessive amounts of computational resources.

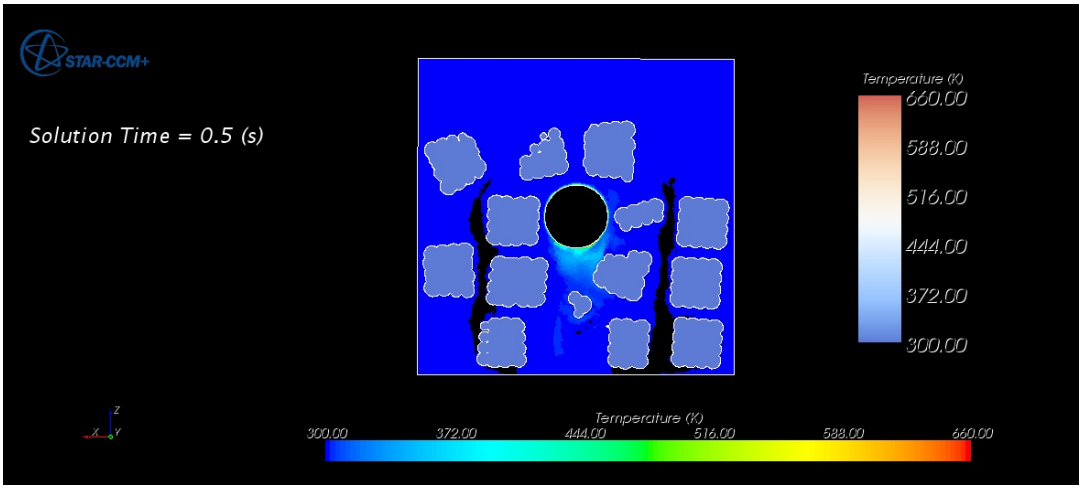

(a) Solution time of 0.5 seconds.

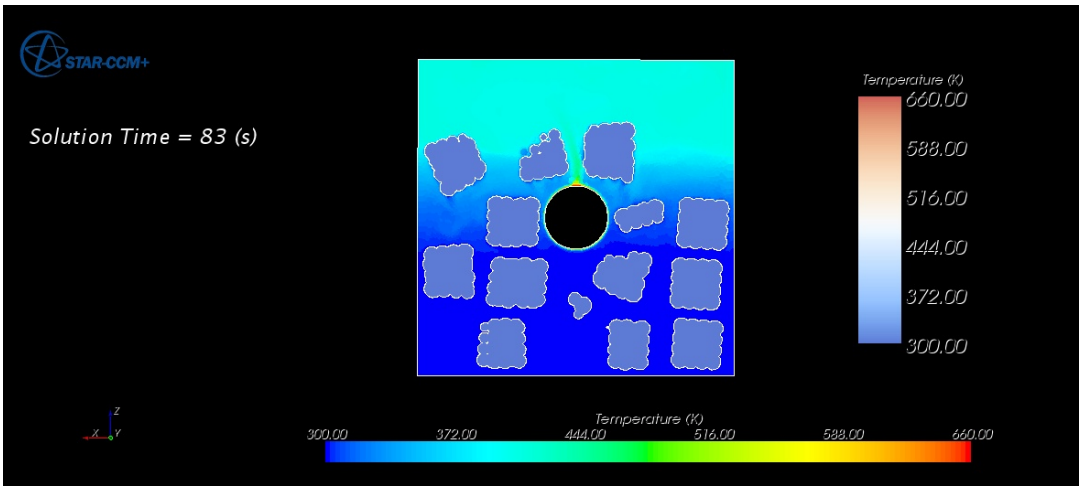

(b) Solution time of 83 seconds.

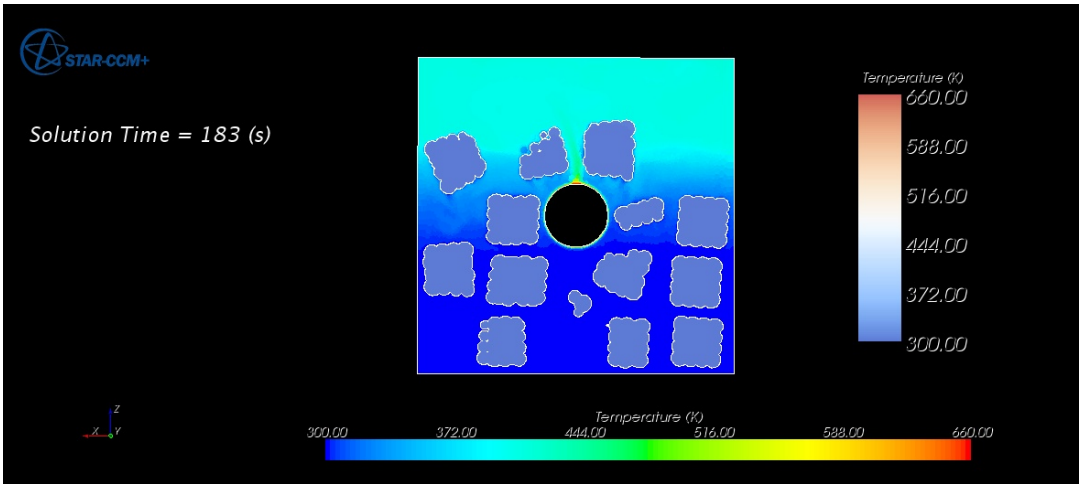

(c) Solution time of 183 seconds.

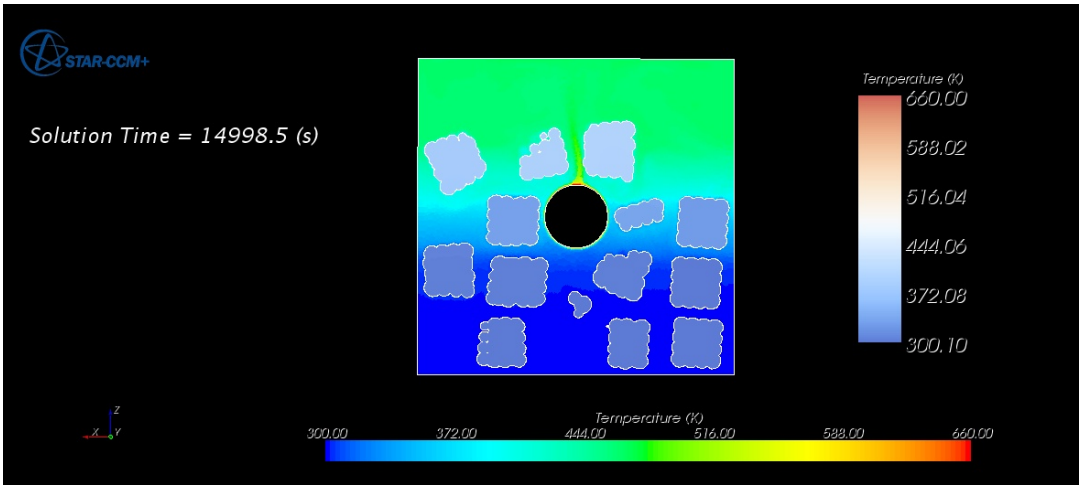

(d) Solution time of 14,998.5 seconds.

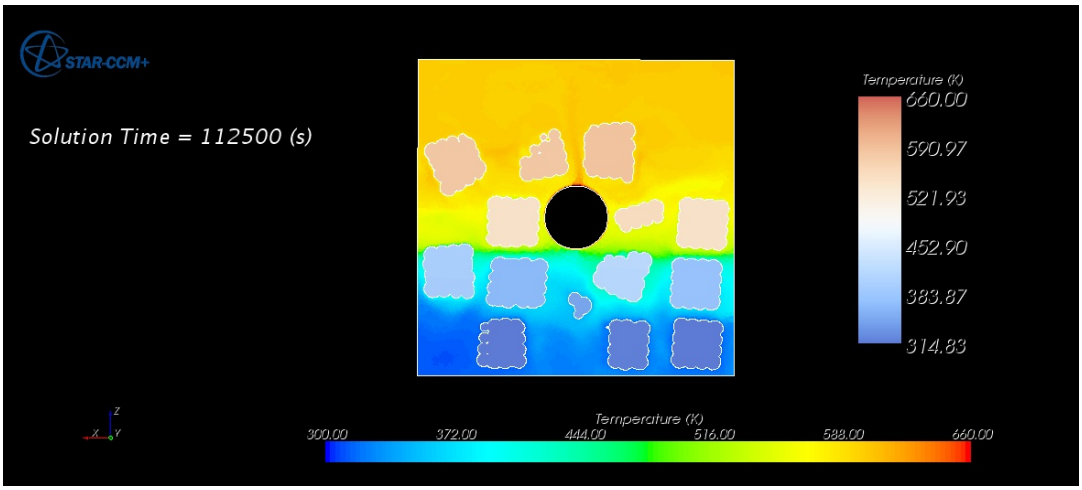

(e) Solution time of 112,500 seconds.

Figure 30. Simulation results obtained using the newly implemented operator splitting algorithm.

CONCLUSIONS

In our research we are taking the novel approach of applying CFD-based simulation tools to a modified in-situ process for the production of oil from oil shale. We are developing a simulation tool that captures the relevant physical processes and data from a large-scale system. Currently we are focusing on pilot-scale heat transfer data obtained from Red Leaf Resources' EcoShale capsule. We have demonstrated the need to understand the fluid flow behavior that occurs in the convective channels in the rubblized shale bed. Heat transfer occurs predominantly through the convective channels, greatly decreasing the time required to heat the oil shale to the production temperature when compared with conductive heating alone.

We have developed and implemented a geometry creation strategy for a representative section of the EcoShale capsule, developed a meshing approach to deal with the complicated geometry and produce a well-behaved mesh, analyzed the effects of boundary conditions on the simulation results, and devised a new operator splitting solution algorithm to take advantage of the differing convective and conductive time scales occurring in the simulation. With the operator splitting algorithm, we have obtained a long-term thermal history of the oil shale particles.

In Phase II of this project we will apply kinetic models to estimate the oil production from our representative computational domain. Once this tool set has shown its efficacy with a demonstration simulation of the representative EcoShale capsule geometry, we will complete a V/UQ analysis involving experimental uncertainty, model uncertainty, operating condition uncertainty and numerical uncertainty with the goal of better understanding the processes that drive production in a modified in-situ process.

REFERENCES

1. Red Leaf Resources, Inc. (n.d.). Available at www.redleafinc.com.

National Energy Technology Laboratory

626 Cochrans Mill Road
P.O. Box 10940
Pittsburgh, PA 15236-0940

3610 Collins Ferry Road
P.O. Box 880
Morgantown, WV 26507-0880

13131 Dairy Ashford, Suite 225
Sugarland, TX 77478

1450 Queen Avenue SW
Albany, OR 97321-2198

2175 University Ave. South
Suite 201
Fairbanks, AK 99709

Visit the NETL website at:
www.netl.doe.gov

Customer Service:
1-800-553-7681